

Single reaction interface in flow analysis

Marta F.T. Ribeiro^a, João L.M. Santos^{a,*}, José L.F.C. Lima^a,
Ana C.B. Dias^b, Elias A.G. Zagatto^b

^a *REQUIMTE, Faculdade de Farmácia da Universidade do Porto, Rua Aníbal Cunha, 164, 4099-030 Porto, Portugal*

^b *Centro de Energia Nuclear na Agricultura, Universidade de S.Paulo, P.O. Box 96, Piracicaba 13400-970, Brazil*

Received 30 May 2005; received in revised form 28 August 2005; accepted 28 August 2005

Available online 7 October 2005

Abstract

The dual or multiple reaction interface concept, commonly associated to the distinct flow techniques, was replaced by a single interface concept, which do not rely on the utilisation of a well-defined and compelling sample volume but only on mutual penetration of sample and reagent zones at a single reaction interface where both sample and reagent met together prior to detection. In the proposed approach basic principles of flow analysis, such as controlled dispersion and reaction zone formation, are not influenced by sample and reagent volumes but determined exclusively by the extension of the overlap of two adjoining quasi-infinite zones enhanced by multiple flow reversals and the pulsed nature of the flowing streams.

The detector is positioned at the core of the flow manifold (not in the conventional terminal position), and repetitive flow reversals enable interface manipulations, including multi-detection of the entire reaction interface or the monitoring of the evolution of a pre-selected interface zone by using suitable reversal cycle times.

The implementation of the developed approach was facilitated due to the configuration simplicity and operational versatility of multi-pumping flow systems. Its performance was evaluated by monitoring processes involving two or four-solution reaction interfaces.

© 2005 Elsevier B.V. All rights reserved.

Keywords: Flow analysis; Single reaction interface; Multi-pumping flow system; Solenoid micro-pump

1. Introduction

The need for simplification of conventional analytical procedures that dictated the inception of flow injection analysis (FIA) [1] has motivated the emergence and subsequent introduction of novel concepts, approaches, techniques and applications. A plethora of FIA alternatives characterised by enhanced ruggedness, reliability or long-term stability have been proposed over the past decades such as sequential injection analysis (SIA) [2], multicommutation [3], multisyringe [4] or multi-pumping [5] flow systems. In the past, pulsed flows [6,7] were always considered a hindrance to be avoided, but nowadays they have been envisaged as beneficial in most of the analytical circumstances. Compactness, considered in terms of fewer components performing identical or increasing number of tasks, and miniaturisation, regarded as reduced dimensioned devices, are expressions progressively more associated to flow-based analytical systems.

Micro-total analytical systems (μ TAS) are receiving an increasingly attention [8,9].

Regardless of the involved flow-based technique, the sample volume is always a key parameter requiring a systematic optimisation. Whether the selected sampling strategy changing the inserted sample volume is an effective strategy to adjust the sensitivity of the determination affecting as well the working concentration range and sampling rate [10,11].

A typical characteristic of almost all flow-based methods is the positioning of the detector at the end of the analytical path, where it provides a single sample measurement that in some analytical circumstances could not be considered sufficient, as it does not convey any kinetic data and/or cannot compensate operational errors. In contrast, the information supplied by multi-detection performed on a single sample zone can be used for e.g. kinetic measurements, multi-analyte determinations, suppression of interfering species, adjustment of sensitivity and/or working analytical range, etc.

Zone penetration was a concept initially proposed by Ruzicka and Hansen [1] to explain the formation of a composite zone when, in two flowing neighbouring solutions, the trailing solu-

* Corresponding author. Tel.: +351 22 2087132; fax: +351 22 2004427.
E-mail address: Joalms@ff.up.pt (J.L.M. Santos).

tion penetrated the leading one as a consequence of the higher than average flow velocity of the central streamlines with respect to the average velocity of the flowing stream. The concept gained an additional relevance with the advent of sequential injection [2,12], which combines zone sequencing and flow reversal to achieve the desired degree of penetration of sample and reagent zones.

In this work, a novel flow-based approach exploiting zone penetration is proposed. Although similar to SIA in the sense that zone penetration influenced dramatically the extension of the surface area over which a sample/reagent concentration gradient is established, it no longer relies on the utilisation of compelling sample and reagent volumes. Consequently, a complete zone overlap is never attainable, as sample and reagent zones have no fixed boundaries. The foundation of the proposed system herein named single interface flow analysis (SIFA) is the establishment of a dynamic single reaction interface, where the sample and reagents are put in contact; further reaction development is then dependent of the mutual sample/reagents interpenetration. Moreover, zone overlap is facilitated by multiple flow reversals and by the pulsed nature of the flowing streams generated by the actuation of the solenoid micro-pumps, which are accountable for solutions insertion and propelling. SIFA exhibits an additional advantage of allowing multiple detection, and was evaluated with two easily implemented manifold configurations: a simpler one that was used to carry out the reaction of Fe(III) with salicylic acid and a more complex, comprising four solenoid micro-pumps, that was assessed in the determination of phosphate involving the molybdenum blue formation.

2. Experimental

2.1. Reagents

All chemicals were of analytical reagent grade, and doubly deionised water (conductivity $< 0.1 \mu\text{S cm}^{-1}$) was used throughout.

The $7.16 \times 10^{-3} \text{ mol l}^{-1}$ Fe(III) stock solution was prepared by dissolving 1.936 g $\text{FeCl}_3 \cdot 6\text{H}_2\text{O}$ in 10 ml of conc. HCl plus 10 ml of conc. HNO_3 , and making the volume up to 1000 ml with water. Working standards within the 1.8 to $9.0 \times 10^{-4} \text{ mol l}^{-1}$ range were prepared by suitable dilutions of the above stock with water.

A $1.45 \times 10^{-2} \text{ mol l}^{-1}$ salicylic acid solution was prepared by dissolving 0.20 g in 10 ml of ethanol and making the volume up to 100 ml with water.

A $5.26 \times 10^{-3} \text{ mol l}^{-1}$ phosphate stock solution was prepared by dissolving 1.201 g $\text{K}_2\text{HPO}_4 \cdot 3\text{H}_2\text{O}$ in 1000 ml of water. Working standard solutions within the 1.0 to $4.0 \times 10^{-4} \text{ mol l}^{-1}$ range were prepared by suitable dilutions of the above stock with water.

A 0.005 mol l^{-1} ammonium heptamolybdate solution was prepared by dissolving 1.236 g $(\text{NH}_4)_6\text{Mo}_7\text{O}_{24} \cdot 4\text{H}_2\text{O}$ in 200 ml of 0.4 mol l^{-1} HNO_3 .

A $5.7 \times 10^{-2} \text{ mol l}^{-1}$ ascorbic acid solution was daily prepared by dissolving 2.0 g of ascorbic acid in 200 ml of water.

2.2. Apparatus

The single interface flow system comprised a set of solenoid micro-pumps (Bio-Chem Valve Inc., Boonton, NJ, USA, 8 or $25 \mu\text{l}$ per stroke) [5], two-way solenoid valves 161 T031 (NRResearch Inc., West Caldwell, NJ, USA), a Jenway 6300 spectrophotometer (Jenway, Dunmow, UK) equipped with a flow-cell (10 mm optical path, 18 or $80 \mu\text{l}$ inner volume), and straight reaction coils and transmission lines made of PTFE tubing (0.8 mm i.d.). Home made end-fittings and connectors were also used.

A Pentium I based computer was used for system control, and for data acquisition and treatment; software was developed in Microsoft Quick-Basic 4.5. The computer equipped with a PC-LABcard model PCL-711B (Advantech) interface card. A home made ULN 2003 based or a CoolDrive (NRResearch Inc.) power drive was used to operate both the solenoid micro-pumps and the valves.

2.3. Single interface flow manifold

The developed approach was evaluated by using two different flow manifolds comprising two (Fig. 1A) or four (Fig. 1B) solenoid micro-pumps depending on the chemical reaction under evaluation. The solenoid micro-pumps were used to insert and to propel the sample and reagent solutions. The repetitive micro-pump switching on/off created a pulsed flowing stream in which the pulse volume corresponded to the micro-pump stroke volume. Two two-way solenoid valves were used in order to direct the streams. The multiple flow reversals were carried out by

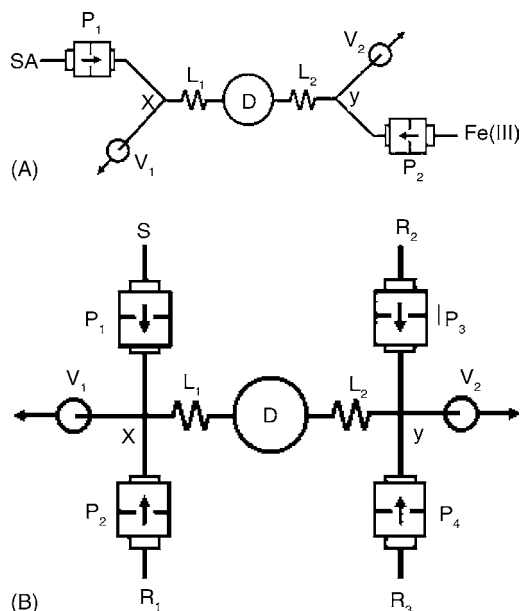


Fig. 1. Single interface flow manifolds. (A) Involving utilisation of two solutions: P₁ and P₂, solenoid micro-pumps; V₁ and V₂, solenoid valves; Fe(III), Iron(III) solution; SA, salicylic acid solution; D, detector; L₁ and L₂, reaction coils; X and Y, confluence points. (B) Involving utilisation of four solutions; P₁, P₂, P₃ and P₄, solenoid micro-pumps; V₁ and V₂, solenoid valves; S, phosphate sample; R₁, ammonium heptamolybdate solution; R₂, ascorbic acid solution; R₃, water; D, detector; L₁ and L₂, reaction coils; X and Y, confluence points.

combined actuation of the solenoid micro-pumps and solenoid valves. The detector was placed at the core of the flow manifold and the micro-pumps and valves were positioned symmetrically around it. Using two identically lengthened reaction coils placed on both sides of the detector complemented this assemblage. In this way, it was possible to carry out multiple detections preceded by symmetrical flow reversals, whose extension was determined by the travelling of the reaction interface within each reactor under a time-base or a pulse-counting control routine.

For the simplest flow manifold (Fig. 1A) involving reaction of Fe(III) with salicylic acid (SA), the analytical cycle was started by establishing a baseline, which could be achieved either with the SA or the Fe(III) solutions. To establish a baseline with SA, V_1 was closed and P_1 was repeatedly actuated (on/off switching) propelling the salicylic acid solution through the reactors L_1 and L_2 as well as through detector. After reaching the confluence point Y, the SA solution was discarded through V_2 , which was kept open. Subsequently, V_2 was closed, V_1 was opened, P_1 was switched OFF and the Fe(III) solution was inserted into the analytical path by means of P_2 actuation. The Fe(III) solution leading edge met then the SA solution at the confluence point Y and propelled it back to V_1 . The mutual inter-dispersion of SA/Fe(III) inside L_2 resulted in an analytical signal, which was measured when the reaction interface passed through the detector into L_1 .

After the first detection, distinct manipulations of the reaction interface, now within L_1 , could be carried out: the reaction interface could be repeatedly moved back and forward between L_2 and L_1 , by using multiple flow reversals (actuations of V_2 , V_1 , P_2 and P_1), which enabled multi-detections of the entire reaction interface or multiple partial detections of a selected portion of the interface; alternatively, the formed reaction interface could be rejected to waste towards V_1 and a new interface could be created at the confluence point X by actuating P_1 (V_2 open and V_1 closed), which would move the Fe(III) solution within L_1 back to L_2 and produce another analytical signal. On the other hand, the initially formed reaction interface could be partially rejected through V_1 and the terminal portion of the interface that remained within L_1 could be reversed to detection assuring either a renewal of the SA solution at the interface if the reaction was not complete (due to a reagent shortage) or a dilution effect if most of the interface have reached completion. In another possible manipulation the interface could be retained within one of the reactors and be subjected to multiple very short flow reversals, by moving it back and forth for 1, 2 or n pulses, before detection, which would contribute to increase both the mutual sample/reagent zones interpenetration and the residence time.

If baseline was initially established with the Fe(III) solution, system operation would be identical, involving the same device synchronisation: when P_2 was operated V_1 was opened, whereas when P_1 was operated the opened valve would be V_2 .

For Fe(III) sample solutions replacement and cleansing, P_2 was actuated and V_2 was opened (V_1 closed). In this way, the solutions would flow immediately to waste bypassing the detector.

The more complex configuration (Fig. 1B) involved the utilisation of 4 micro-pumps and was evaluated in the determination

of phosphate. P_1 , P_2 and P_3 were used to insert the sample (phosphate), ammonium heptamolybdate and ascorbic acid solutions, respectively. P_4 was used to insert an inert solution (water) in order to guarantee a symmetrical manifold configuration assuring similar flow rates during the two reversal stages. P_4 could also have been used as a dilution promoting micro-pump for the analysis of highly concentrated samples. Nevertheless, utilisation of P_4 was not essential as the flow could be equilibrated by increasing the operational frequency of P_3 .

Analogously to the simpler configuration (Fig. 1A), operation of the flow system was dependent on the synchronisation of two arbitrarily selected consecutive phases. During one of the phases (phase 1), V_1 was closed, V_2 was opened and P_1 and P_2 were simultaneously operated in order to fill the reaction coils L_1 and L_2 as well as the flow cell with a flowing stream resulting from merging of the phosphate and the heptamolybdate solutions. This flowing stream was directed towards waste through V_2 . During next phase (phase 2), V_1 was opened V_2 was closed and the simultaneous operation of P_3 and P_4 generated a flowing stream of ascorbic acid that met the phosphate/heptamolybdate mixture at the confluence point Y driving it back to L_1 through L_2 and through the flow cell where the reaction products formed at the moving interface produced the analytical signal. Subsequently, the interface within L_1 could be subjected to the same manipulations previously referred, like multiple flow reversals (with or without detection), partial reversals, reagent renewal, etc.

3. Results and discussion

Analogously to other flow systems, SIFA is intrinsically a kinetic process depending on two complementary phenomena: the kinetic physical process of sample/reagent mutual inter-dispersion and the reaction chemical kinetics. However, when a fixed sample volume is used, even if physical equilibrium is not reached, a chemical equilibrium can be attained providing that the mean residence time and the reagent amount are properly dimensioned. This explains why peak height often decreases and sample zone spreads out when too long reaction coils are used; a dilution effect prevails over reaction completeness. Moreover, for long residence times dispersion is controlled primarily by the diffusion processes and the peak tends to assume a symmetrical Gaussian shape.

In SIFA, none of the above mentioned equilibria is attained: as the residence time increased and physical zone penetration advances, a sample/reagent gradient is established along the entire span of the reaction interface with point-to-point variable sample/reagent ratio between two confining pure sample (C_A) and reagent sections (C_B) (Fig. 2). If enough residence time is provided certain portions of the interface reach chemical equilibrium, which would correspond to the highest yield of product formation (P) [2], thus to the highest analytical signal (Fig. 3A). A further increase of the residence time would result in an enlargement of the interface as the reaction is conveyed to the neighbouring zone guaranteeing a permanent surplus of sample and reagent. However, despite this increase in the residence time peak height is kept constant, even if very long coils

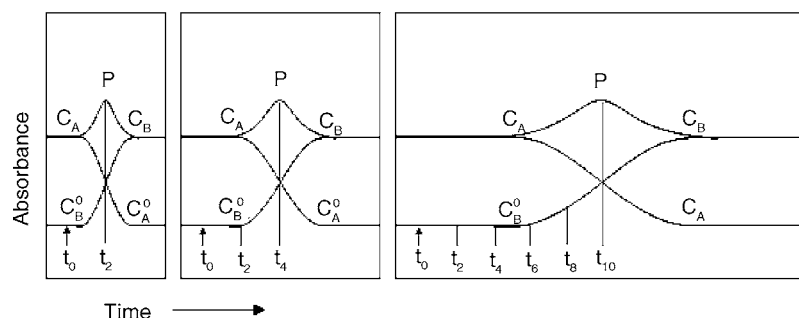


Fig. 2. Scheme of the evolution of the concentration gradient vs. residence time at the single reaction interface. C_A , pure component A; C_B , pure component B; C_A^0 and C_B^0 , components A and B zero concentration limits; P, reaction product.

are used, although the peaks become wider (Fig. 2). For slower reactions (Fig. 3B), the increase in residence time results in an increase of peak height that, as in the previous case, become levelled but broader after the central zone of the interface have reached completion. Reaction zone homogenisation, an objective of conventional flow methods, is therefore never attained. Consequently, the undesirable dilution effect observable in certain conventional flow experiments due to oversized sample dispersion is highly unlikely to occur in SIFA.

3.1. Single detection

By using the flow manifold in Fig. 1A, evaluation of the influence of the residence time on a single detection was carried out by using different reaction coil lengths. Flow rate was set at 0.8 ml min^{-1} and an $18\text{-}\mu\text{l}$ inner volume flow cell was used. For propelling the single reaction interface both

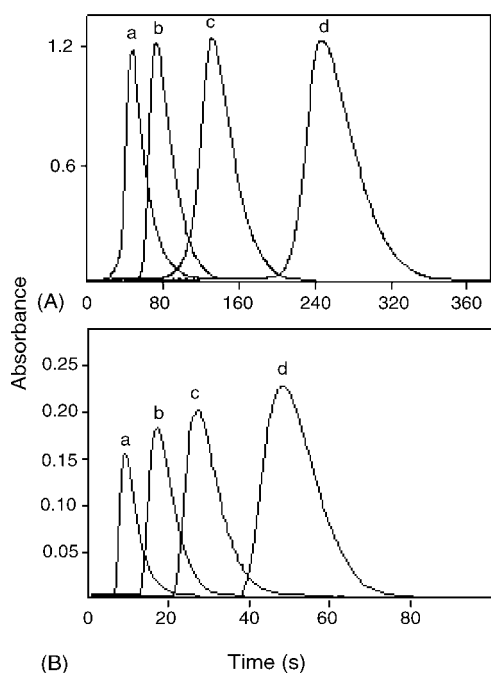


Fig. 3. Influence of lengths of the reaction coils. (A) Refers to the SA–Fe reaction: a (50 cm), b (100 cm), c (200 cm) and d (400 cm) and (B) refers to the molybdenum blue forming reaction: a (10 cm), b (50 cm), c (100 cm) and d (200 cm).

$1.45 \times 10^{-2} \text{ mol l}^{-1}$ SA and Fe(III) solutions at distinct concentrations (1.8 to $9.0 \times 10^{-4} \text{ mol l}^{-1}$) were used. It was verified (Fig. 4B) that peak width at baseline was larger when the interface trailing solution was Fe(III). On the other hand, when Fe(III) was used as carrier, peak height increased up to a coil length of 100-cm and subsequently stabilised, whereas when SA was the carrier the highest analytical signal was obtained with a 200-cm reactor after which it approached stabilisation. In both experiments peak width increased with Fe concentration. Moreover, peak shape was markedly different whether the carrier was SA or Fe(III), namely in terms of peak appearance time, which

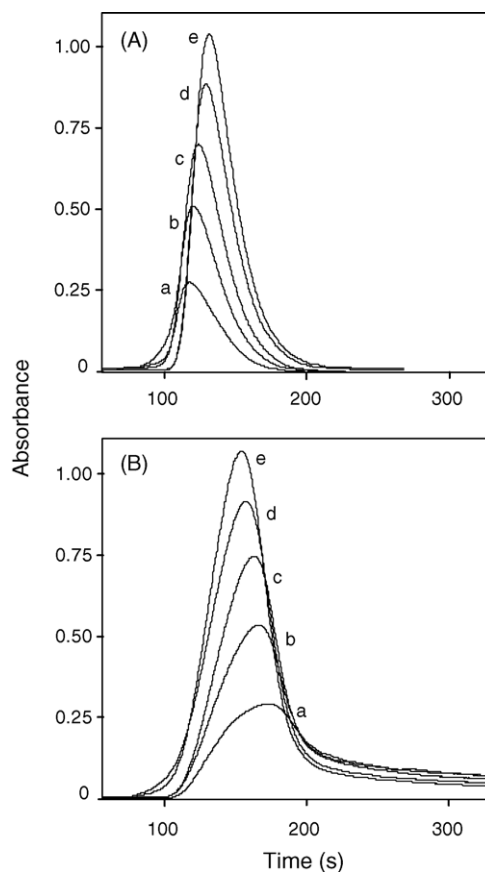


Fig. 4. Influence of Fe(III) concentration. Refers to $1.45 \times 10^{-2} \text{ mol l}^{-1}$ SA; a ($1.8 \times 10^{-4} \text{ mol l}^{-1}$ Fe), b ($3.6 \times 10^{-4} \text{ mol l}^{-1}$ Fe), c ($5.4 \times 10^{-4} \text{ mol l}^{-1}$ Fe), d ($7.2 \times 10^{-4} \text{ mol l}^{-1}$ Fe) and e ($9.0 \times 10^{-4} \text{ mol l}^{-1}$ Fe). (A) and (B) SA or Fe(III) used as trailing solution. A 2-m reaction coil was used.

occurred earlier when the carrier was SA. Furthermore, when SA was the trailing solution the time of maximum detection increased with Fe concentration (Fig. 4A), whereas when Fe(III) was the interface trailing solution, the time of maximum detection increased as the Fe(III) concentration decreased (Fig. 4B). The peak shapes in Fig. 4A and B reveal that the highest analytical signal, corresponding to the isodispersion point [13], was closer to the more concentrated solution participating in the interface (SA) independently of the used trailing solution. As the concentration of Fe(III) increased, decreasing the SA/iron concentration ratio, the isodispersion point shifted towards the Fe(III) solution. It was also observed that the micro-pump stroke volume (8 or 25- μ l) did not affect significantly the results, except for the stair-like shape of the peak contour. Additionally, the maximum detection occurred slightly earlier for a 25- μ l micro-pump when the carrier was SA. The relatively long residence times of Fig. 4 are explained by the utilisation of a long reaction coil (2 m) and the low flow rate (0.8 ml min⁻¹).

Influence of SA concentrations (3.6 to 18.0×10^{-3} mol l⁻¹) on the peak shape was also investigated for a 5.4×10^{-4} mol l⁻¹ Fe(III). It was observed that, contrasting with the previous experiment, peak height was not extensively affected by SA concentration increment even when a 4-m reaction coil was used (increasing markedly the residence time), which was explained by the already initially high SA/iron ratio (Fig. 5). Similarly, changes in peak shape were not so pronounced, especially when SA was the trailing solution. However, minor shifts in the isodis-

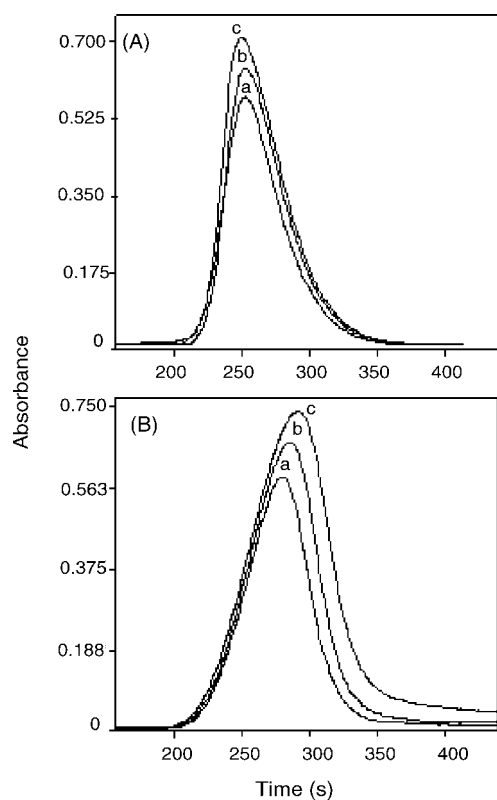


Fig. 5. Influence of SA concentration. Refers to 5.4×10^{-4} mol l⁻¹ Fe(III); a (3.6×10^{-3} mol l⁻¹ SA), b (7.2×10^{-3} mol l⁻¹ SA) and c (18.0×10^{-3} mol l⁻¹ SA). (A) and (B) SA or Fe(III) used as trailing solution. A 4-m reaction coil was used.

person point were noted (Fig. 5), either when SA or Fe(III) were the carrier solutions, and occurred in the direction of the SA solution.

The analytical performance of the developed flow approach was also evaluated. Linear calibration plots for Fe(III) concentrations up to 50 mg l⁻¹ were obtained, either when Fe(III) or SA were used as carrier solution. The calibration curves equations were very similar in both circumstances and were described by $A = 0.0205C + 0.0292$, with a correlation coefficient of 0.996 ($n = 6$), when SA was the carrier and by $A = 0.0215C + 0.0471$, with a correlation coefficient of 0.990 ($n = 6$), when the carrier was Fe(III); A = absorbance and C = concentration in mg l⁻¹.

Regarding the flow manifold in Fig. 1B, it was used to investigate the behaviour of a reaction interface involving four solutions. Actually, the four solutions were previously merged into two flowing streams, which could be individually considered as two solutions that met at the single interface. The studied reaction consisted on the formation of molybdenum blue upon reaction of phosphate with heptamolybdate in the presence of ascorbic acid. Since it was decided to establish a symmetrical flow manifold that would enable the utilisation of identical pulse frequencies on both phases (directions) of the reversing process, a fourth micro-pump (used to introduce water) was added to the system. In these experiments, a 5.0×10^{-3} mol l⁻¹ ammonium heptamolybdate solution, a 5.7×10^{-2} mol l⁻¹ ascorbic acid solution, and increasing phosphate concentrations (1.0 to 4.0×10^{-4} mol l⁻¹) were used.

Evaluation of the analytical signals obtained with a single detection by using reaction coils within 10 and 200 cm showed that peak height increased with the residence time, either when the interface trailing solution was heptamolybdate (HM)/phosphate (P) or ascorbic acid (AA)/water (W), which confirmed the slower kinetics of the reaction when compared with the salicylic acid/Fe(III) one. On the other hand, peak height was slightly higher when HM/P was the trailing solution (the difference in peak height obtained by using HM/P or AA/W as trailing solutions increased with phosphate concentration). However, it was observed that this peak height divergence decreased as the length of the reaction coil increased. In terms of peak profile, it was verified that maximum detection was attained noticeably faster when the carrier was AA/W (for a 100-cm reactor peak maximum was achieved at about 27 s) and that the isodispersion point was not affected by the increment in phosphate concentration (Fig. 6B). Similar isodispersion point behaviour was observed when HM/P was the interface trailing solution although the peaks exhibited a more Gaussian shape (Fig. 6A). Peak maximum was achieved at about 40 s.

In terms of analytical performance linear calibration plots for phosphate concentrations up to 40 mg l⁻¹ were obtained regardless of the carrier solution being used. When HM/P was the trailing solution a typical analytical curve was described by $A = 0.0116C + 0.0082$, with a correlation coefficient of 0.998 ($n = 5$), while when the carrier was AA/W the analytical curve was represented by $A = 0.0102C + 0.001$, with a correlation coefficient of 0.999 ($n = 5$); A = absorbance and C = concentration in mg l⁻¹.

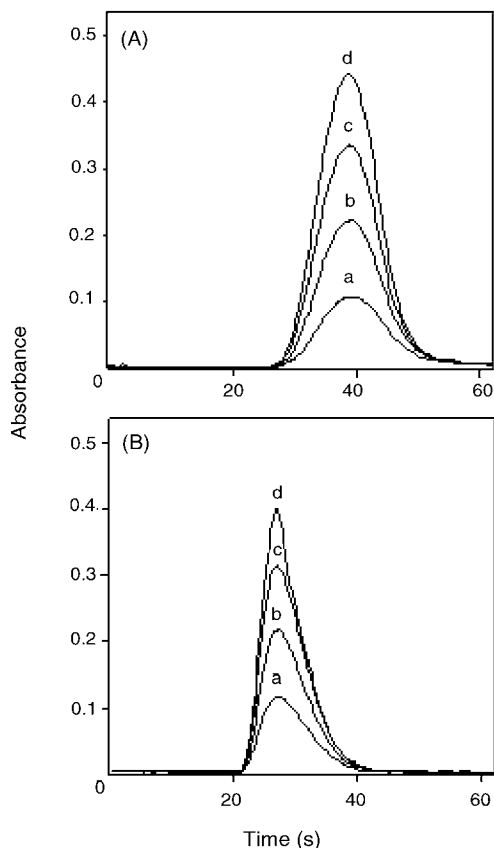


Fig. 6. Influence of phosphate concentration. Refers to $5.0 \times 10^{-3} \text{ mol l}^{-1}$ heptamolybdate; a ($1.0 \times 10^{-4} \text{ mol l}^{-1}$ phosphate), b ($2.0 \times 10^{-4} \text{ mol l}^{-1}$ phosphate), c ($3.0 \times 10^{-4} \text{ mol l}^{-1}$ phosphate) and d ($4.0 \times 10^{-4} \text{ mol l}^{-1}$ phosphate). (A) and (B) Heptamolybdate/phosphate or ascorbic acid/water used as trailing stream. A 1-m reaction coil was used.

3.2. Flow reversal

The flow reversal creates a composite interface zone given that the sample and reagent zones penetrate each other owing to combined effects of axial and radial dispersion. As the number of flow reversals increase the interface stretched out and the reaction is conveyed to adjoining regions increasing the width of the product zone [14,15], which is subsequently measured at the detector.

The reversal of the flow direction, controlled either on a time-based or on a pulse-counting routine, could be carried out

by allowing the entire reaction interface to pass through the detector flow cell, on an analytical signal baseline-to-baseline approach, or by selecting a specific zone of the reaction interface which is repeatedly sampled back and forward so all measurements take place within no return to baseline. In this way, the multiple consecutive detections could provide valuable kinetic data of the entire reaction interface or could be used to establish the kinetic profile of a specific zone. Alternatively, flow reversal could take place within the reaction coil previous to detection. This strategy could be used to increase the reaction time likewise the stopped-flow approach. However, it exhibits a noteworthy advantage regarding the later because it assures a continuous uninterrupted sample/reagent mixing (with no significant dilution effect), while in the stopped-flow approach the mixing of sample and reagent ceases when the flow is halted. Accordingly, multiple very short flow reversals at a define site of the flow manifold contribute to an increase of the mixing efficiency and thus to a faster reaction development while the increased residence time enabled the reaction to reach completion.

Evaluation of the influence of multiple flow reversals on the reaction between SA and iron was carried out by complete reversal of the interface after return of the analytical signal to baseline (Fig. 7). The analysis of the obtained peaks showed that when SA was the trailing solution peak height (b) was slightly lower than when Fe(III) was used (a). This could be explained as a Schlieren disturbance arising from the parabolic interface shape and the different concentration gradient between both solutions. Nevertheless, we have changed the direction of the solutions entering the flow cell, which resulted in the reversion of the concentration gradient traversed by the light beam, but the peak height discrepancy persisted. Another interesting observation was that peak width at baseline was much higher when Fe(III) was the trailing solution. Effectively the peak residence time (baseline-to-baseline) was around 180 s when Fe(III) was the trailing solution and about 90 s when the trailing solution was SA. Moreover, peak width slightly increased as the number of flow reversals increased when the carrier was Fe(III) and remained unchanged when SA was used. Peak height was not affected by the increase in the residence time provided by the consecutive flow reversals, even if peak width increased, because the reaction at the central zone of the interface had already reached completion.

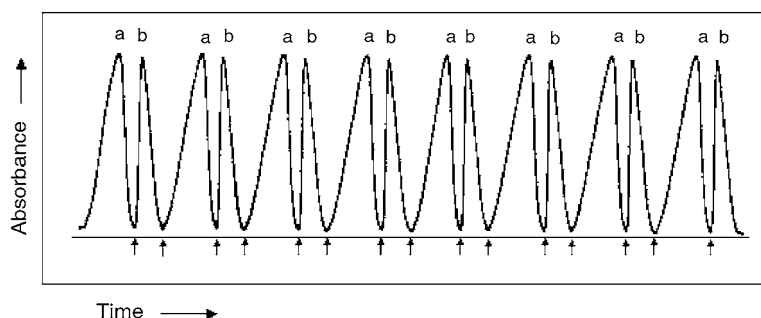


Fig. 7. Multiple (16) flow reversals of the reaction interface SA/Fe(III). Small arrows within graphic represent the point of flow (interface) reversal. Peaks (a) and (b) Fe(III) or SA used as trailing solution. The residence time (baseline-to-baseline) of (a) and (b) peaks was about 180 s and 90 s, respectively.

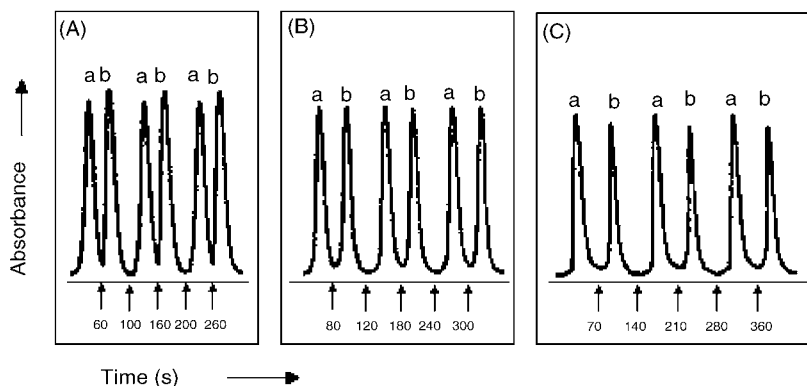


Fig. 8. Influence of the reversal time on the reaction interface between heptamolybdate/phosphate and ascorbic acid/water. (A) Reversal time of 50 s. (B) Reversal time of 60 s. (C) Reversal time of 70 s. Peaks (a) and (b) heptamolybdate/phosphate or ascorbic acid/water used as trailing stream.

The evaluation of the influence of consecutive flow reversals on the phosphate molybdenum reaction was carried out on a time-based routine. The direction of the flowing solutions, thus of the reaction interface, was reverted after 50, 60 and 70 s (Fig. 8). A primary evaluation showed that peak width at baseline was similar whether the propelling solutions were HM/P or AA/W. However, when the solutions direction was reverted after 50 s (Fig. 8A) the peaks obtained using AA/W as trailing solution (b) were higher than those obtained when HM/P was used (a). With a 60 s reversing time (Fig. 8B) peaks were identical, while with a reversing time of 70 s (Fig. 8C) the peaks obtained with HM/P (a) were higher than those obtained with AA/W (b). Apparently, an increase in the residence time resulted in a decrease of the peak height when AA/W was the trailing solution, while the peak height obtained by using HM/P as the propelling solution remained almost unaffected for all the assayed reversing intervals.

An advantageous feature of the developed flow strategy is the possibility of carrying out multiple flow reversals at a specific location of the flow manifold prior to detection. This could be useful when slow reactions are involved since it would enable the increment of the residence time thus of the reaction time without a loss in the sensitivity. In effect, instead of using longer coils or a stopped-flow approach, which would either increase the dispersion or restrain the sample/reagent mixing, it is possible to perform the reversal of the reaction interface for a given number of cycles and for a given reversion degree, which would provide an adequate reaction development prior to detection.

4. Conclusions

Although resembling SIA in the way that sample and reagents are mixed, SIFA differs in important aspects as is the case of not need a holding coil, which in SIA is lengthened to prevent penetration of the front section of the sample zone into the propelling device thus avoiding problems with cross-contamination. In effect, any section of the interface that could not be contained within the analytical path is sent to waste through V_1 or V_2 . Furthermore, the extension of mutual zone penetration could be controlled either by the length of the reaction coils or by

the multiple more or less stretched out flow reversals (in both directions) that could be carried at a definite site within the reaction coils. Moreover, SIFA benefits from the multi-pumping flow systems (MPFS) potential because the pulsed nature of the flowing stream is an inherent advantage of the proposed system in terms of mixing efficiency. Finally, all solutions are propelled under positive pressure, while in SIA sample and reagents are aspirated into the holding coil. On the other hand, the importance of manipulating parameters such as coil length, sample volume and flow rate to obtain the required degree of dispersion is minimised and a more easily implemented and controlled flow system is obtainable. Nevertheless, the versatility and simplicity of operations of MPFS facilitate any run-time adjustment, if required.

Contrasting with the almost Gaussian-shaped analytical signals obtained in consecutive detections in flow analysis, in the developed approach all peaks exhibit a typical shape although they become broader as the number of detections increased revealing that the extent of the reaction interface increased as well. However, whereas in FIA the increment of peak width at baseline is accompanied by a reduction in peak height, as sample dispersion prevails, in the developed flow strategy peak height remains constant and is unaffected by the number of flow reversals, which did not impair sensitivity.

The possibility of carrying out multiple reaction zone detections, in a simple and expeditious way, is a noteworthy advantage of SIFA, because it enables the gathering of an array of data (of the whole interface or of a specific section) without a loss in sensitivity, which could be useful in many aspects in the implementation of automated methods of analysis, namely in terms of kinetic approaches, multi-components analysis, interference suppression, etc.

The developed flow approach exhibited a very high reproducibility even taking into consideration that the reaction takes place at an interface with steep concentration gradients. Naturally, these concentration gradients are attenuated as the reaction proceeds and dispersion increases, but even when short reaction coils were used precision was noteworthy. These results confirmed the reproducibility of zone penetration, either for two or four solutions' reactions, independently of the used trailing solution.

Acknowledgements

The authors thank the consortium agreement CNPq (Brazil)/GRICES (Portugal). M.F.T. Ribeiro thanks FCT and FSE (III QCA) and A.C.B. Dias thanks FAPESP for the PhD grants.

References

- [1] J. Ruzicka, E.H. Hansen, *Anal. Chim. Acta* 78 (1975) 145.
- [2] J. Ruzicka, G.D. Marshall, *Anal. Chim. Acta* 237 (1990) 329.
- [3] B.F. Reis, M.F. Giné, E.A.G. Zagatto, J.L.F.C. Lima, R.A.S. Lapa, *Anal. Chim. Acta* 293 (1994) 129.
- [4] V. Cerdá, J.M. Forteza, A. Cladera, E. Becerra, P. Altimira, P. Sitjar, *Talanta* 50 (1999) 695.
- [5] R.A.S. Lapa, J.L.F.C. Lima, B.F. Reis, J.L.M. Santos, E.A.G. Zagatto, *Anal. Chim. Acta* 466 (2002) 125.
- [6] E.B. van Akker, M. Bos, W.E. van der Linden, *Anal. Chim. Acta* 378 (1999) 111.
- [7] P.S. Francis, S.W. Lewis, K.F. Lim, K. Carlsson, B. Karlberg, *Talanta* 58 (2002) 1029.
- [8] A. Manz, N. Graber, H.M. Widmer, *Sens. Actuators B* 1 (1990) 244.
- [9] K. Huikko, R. Kostianen, T. Kotiaho, *Eur. J. Pharm. Sci.* 20 (2003) 149.
- [10] J. Ruzicka, E.H. Hansen, *Flow Injection Analysis*, second ed., Wiley, New York, 1988.
- [11] M. Trojanowicz, *Flow Injection Analysis: Instrumentation and Applications*, first ed., World Scientific, London, 2000.
- [12] T. Gubeli, G.D. Christian, J. Ruzicka, *Anal. Chem.* 63 (1991) 2407.
- [13] J.F. van Staden, H. Plessis, S.M. Linsky, R.E. Taljaard, B. Kremer, *Anal. Chim. Acta* 354 (1997) 59.
- [14] J.F. van Staden, A. Botha, *S. Afr. Tydskr. Chem.* 51 (1998) 100.
- [15] A. Rios, M.D. Luque de Castro, M. Valcárcel, *Anal. Chem.* 60 (1988) 1540.